[Electronic Supplementary Information]

Theoretical Insights into Single-Atom Catalysts for Improved Charging and Discharging Kinetics of Na-S and Na-Se Batteries

Mukesh Jakhar,*,†,‡ Veronica Barone,*,†,‡ and Yi Ding¶

† *Science of Advanced Materials Program, Central Michigan University, Mt. Pleasant, MI 48859, USA*

‡*Department of Physics, Central Michigan University, Mt. Pleasant, MI 48859, USA*

¶ *U.S. Army DEVCOM-GVSC, Warren, MI 48397, USA*

E-mail: jakha1m@cmich.edu; baron1v@cmich.edu

Table of Contents

Electronic properties of g−C_3N_4 and phonon spectrum curves for SA@rg−C_3N_4

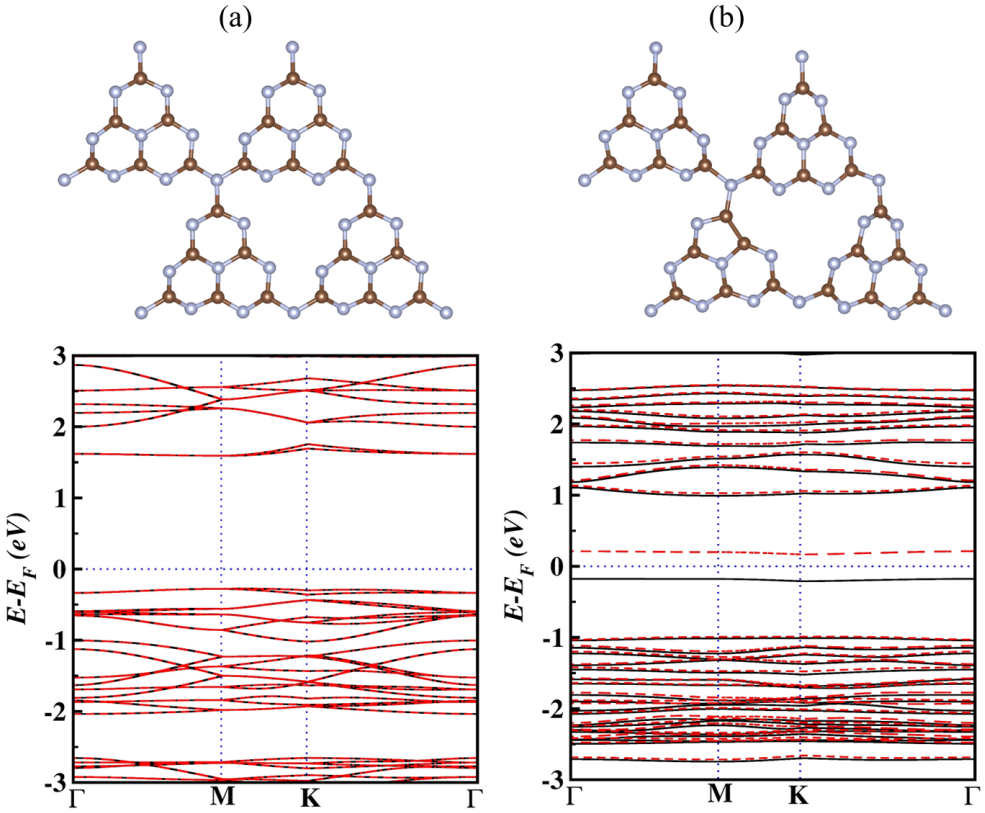

Figure S1: The optimized configuration and electronic band structure for (a) g−C_3N_4 and rg−C_3N_4 monolayer. Solid black and dotted red curves are spin-down and spin-up components, respectively. Fermi level is set to zero.

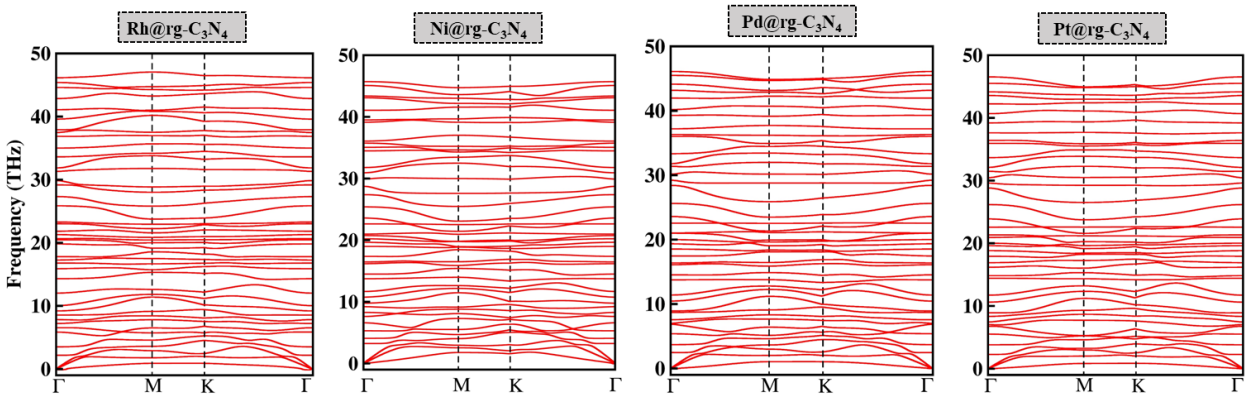

Figure S2: Phonon spectrum curves of SA@rg$-C_3N_4$ (for SA= Rh, Ni, Pd, and Pt)

Table S1: The average bond lengths between the embedded single atom (SA) and its nearest neighboring N and C atoms within the 1 x 1 unit cell of a rg$-C_3N_4$ monolayer.

SA	SA-N (Å)	SA-C (Å)
Co	1.90	1.76
Fe	1.93	1.79
Ir	2.04	1.87
Ni	1.90	1.81
Pd	2.02	1.92
Pt	2.01	1.91
Rh	2.03	1.86

Charge Transfer and AIMD plot for X_8 (X= S, Se) Species

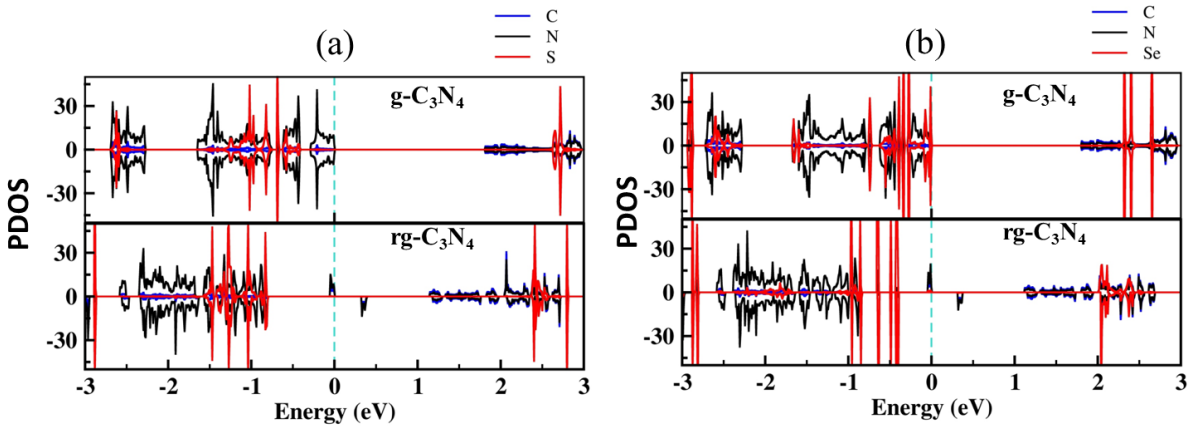

Figure S3: The calculated partial density of states (PDOS) for g$-C_3N_4$ and rg$-C_3N_4$ absorbed by (a) S_8 and (b) Se_8 molecules

From Figure S3, it is evident that in g$-C_3N_4$ absorbed by S_8, there is a predominant contribution from N atoms near the Fermi level. However, in Se_8, in addition to the N atom contribution, a significant contribution from Se atoms is also observed, which can be correlated to their higher adsorption energies compared to S_8. On other hand, in rg$-C_3N_4$, only two small N atom peaks occur near the Fermi level corresponding to spin up and spin down, which can be correlated to their lower adsorption energies compared to pristine g$-C_3N_4$.

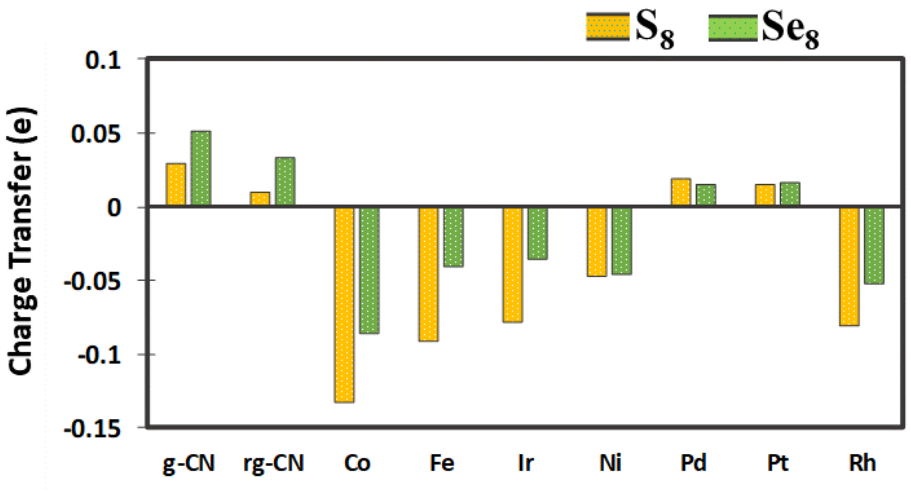

Figure S4: The charge transfer between the X_8 (X= S, Se) molecules and various substrates.

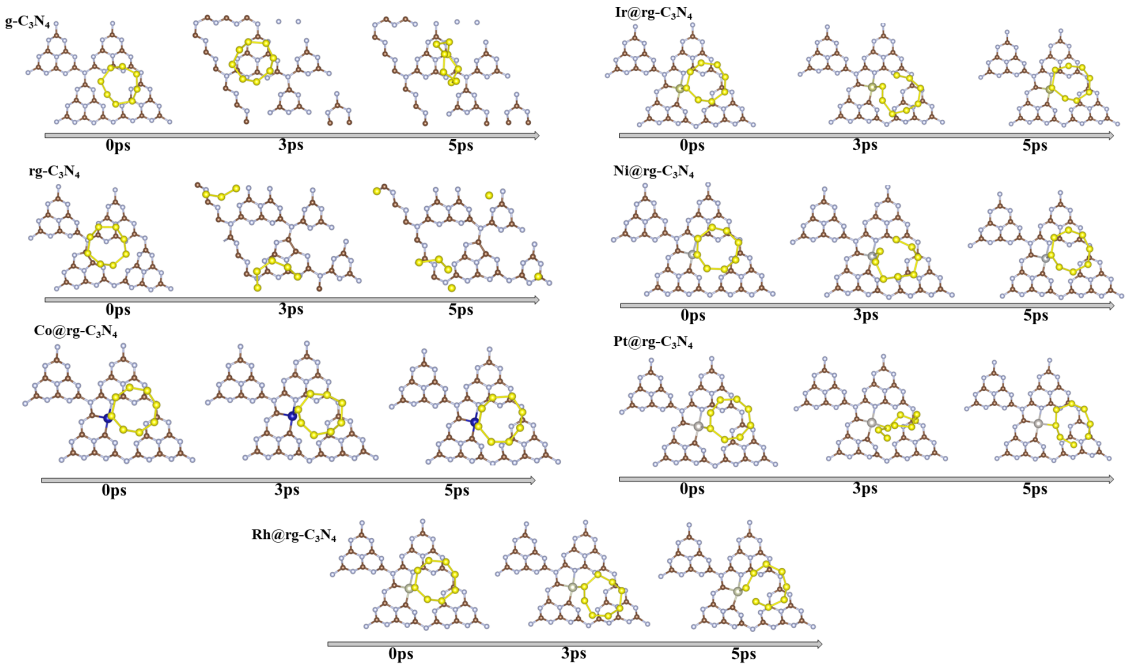

Figure S5: AIMD simulation snapshots of the adsorption of S_8 on g$-C_3N_4$, rg$-C_3N_4$, and SA@rg$-C_3N_4$ (SA = Co, Ir, Ni, Pt, and Rh)

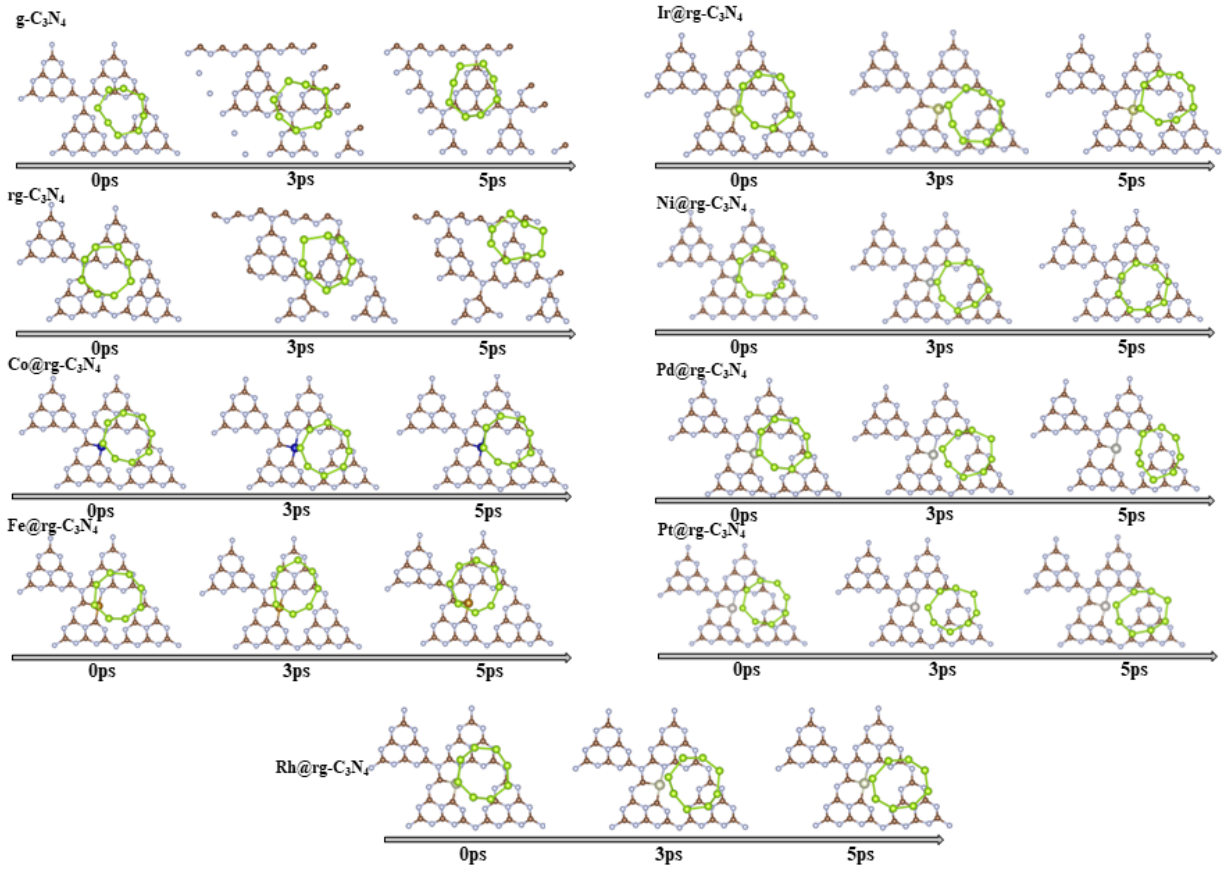

Figure S6: AIMD simulation snapshots of the adsorption of Se_8 on g$-C_3N_4$, rg$-C_3N_4$, and SA@rg$-C_3N_4$ (SA = Co, Fe, Ir, Ni, Pd, Pt, and Rh)

Geometric Configurations of Na-pXs (X=S, Se)

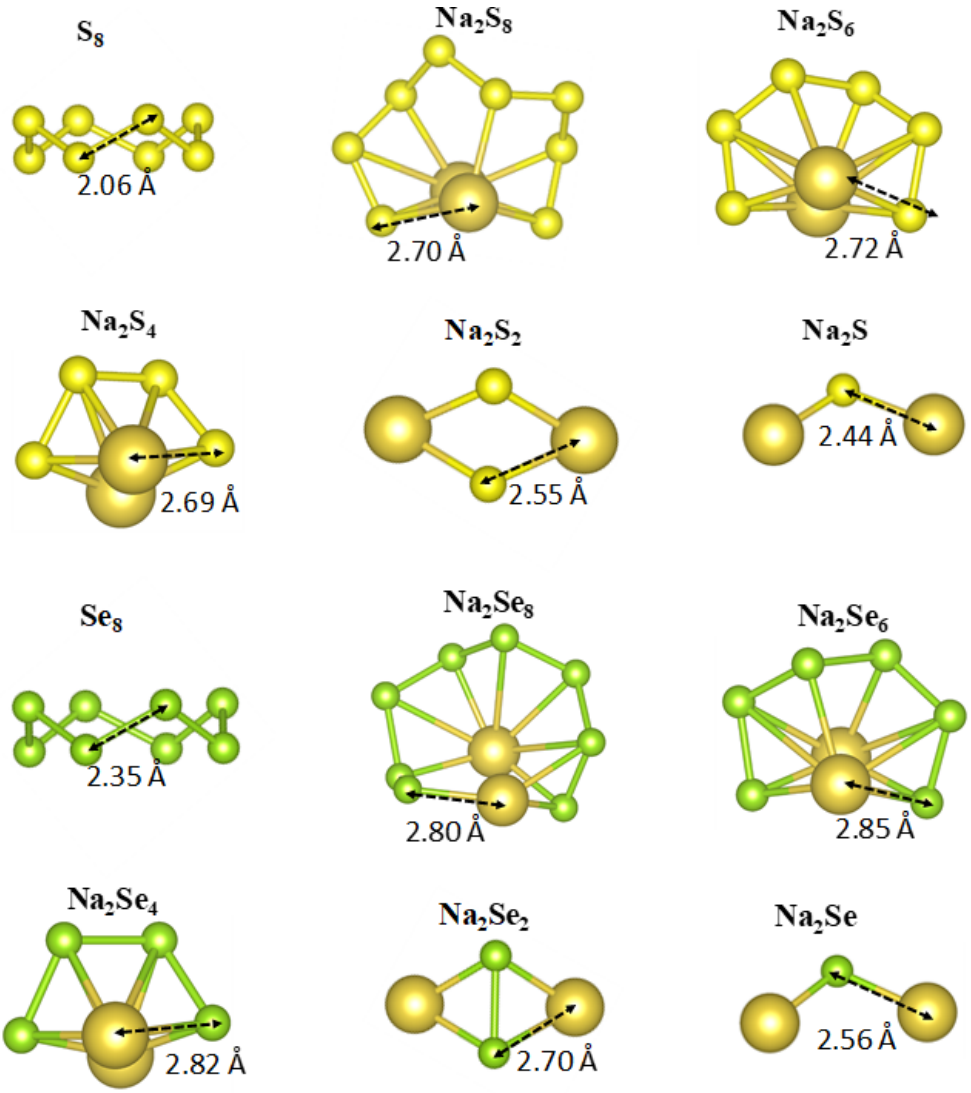

Figure S7: The optimized geometric configurations of X_8 (X= S, Se) and Na_2X_n (n=1, 2, 4, 6, 8) species.

Table S2: The bond lengths between the Na atom and its nearest neighboring X (X=S, Se) atom within the Na-pXs species.

Na-pXs (X=S, Se)	Na-S (Å)	Na-Se (Å)
N_2X	2.44 (2.44)[a]	2.56 (2.57)[b]
Na_2X_2	2.55 (2.56)[a]	2.70 (2.70)[b]
Na_2X_4	2.69 (2.71)[a]	2.82 (2.83)[b]
Na_2X_6	2.72 (2.72)[a]	2.85 (2.86)[b]
Na_2X_8	2.70 (2.76)[a]	2.80 (2.81)[b]

*Here a and b represent the reference number[1] and[2] for Na-S and Na-Se bond lengths, respectively.

Table S3: The calculated charge transfer e^- from Na_2X_n (n=1, 4, 8 and X=S, Se) to the rg$-C_3N_4$ and SA@rg$-C_3N_4$ (SA= Co, Fe, Ir Ni, Pd, Pt, and Rh) monolayer.

Systems	Na_2S	Na_2Se	Na_2S_4	Na_2Se_4	Na_2S_8	Na_2Se_8
g$-C_3N_4$	0.81	0.81	0.76	0.51	0.09	0.14
rg$-C_3N_4$	0.86	0.86	0.85	0.85	0.46	0.52
Co	0.66	0.71	0.33	0.37	0.19	0.21
Fe	0.61	0.65	0.29	0.33	0.17	0.19
Ir	0.69	0.75	0.40	0.47	0.25	0.33
Ni	0.63	0.68	0.38	0.42	0.23	0.30
Pd	0.61	0.66	0.36	0.40	0.26	0.32
Pt	0.68	0.73	0.43	0.48	0.31	0.32
Rh	0.65	0.69	0.35	0.41	0.22	0.28

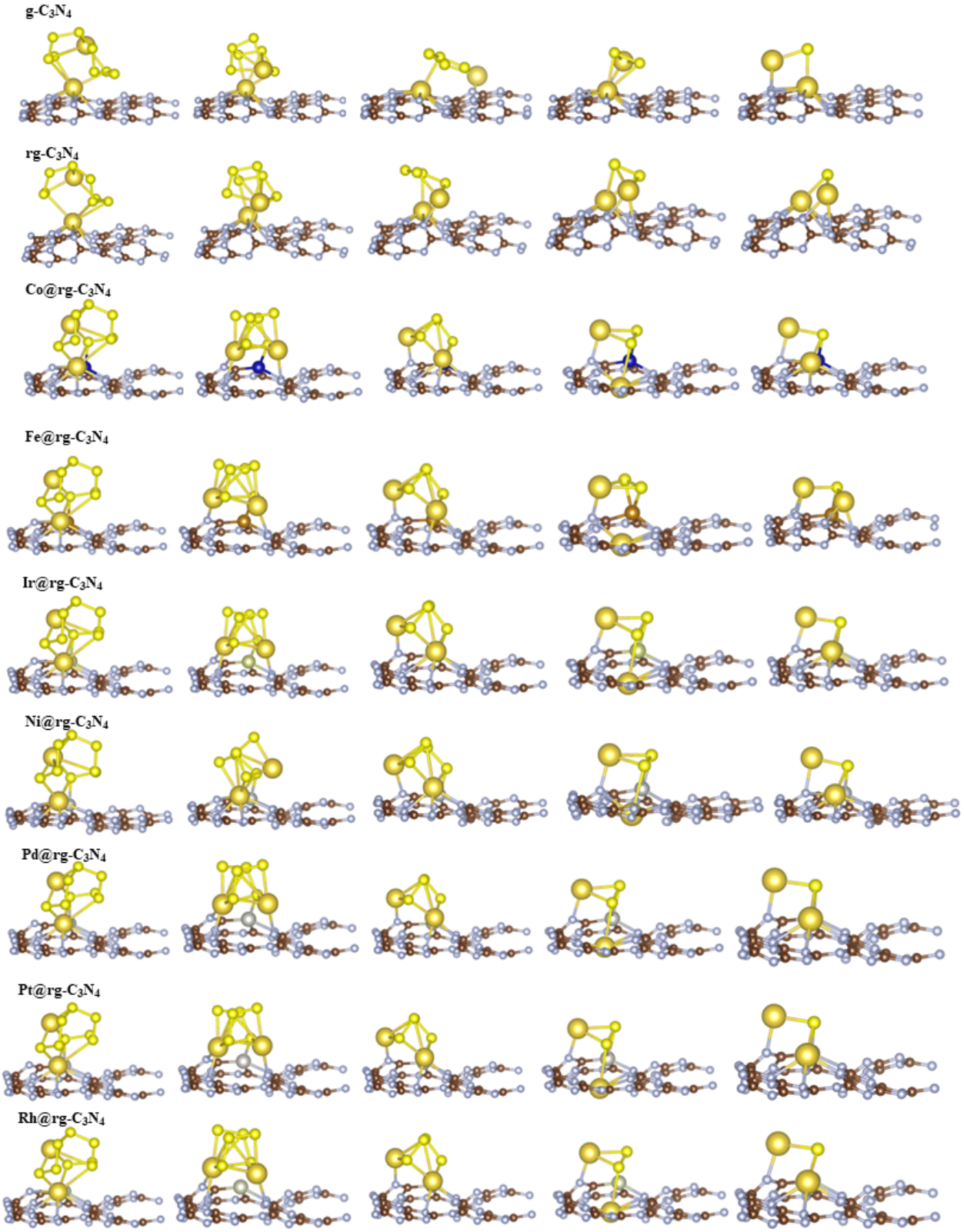

Figure S8: The optimized geometric configurations of Na_2S_n; n=1, 2, 4, 6, 8 species ong$-C_3N_4$, rg$-C_3N_4$ and SA@rg$-C_3N_4$ (SA = Co, Fe, Ir, Ni, Pd Pt and Rh)

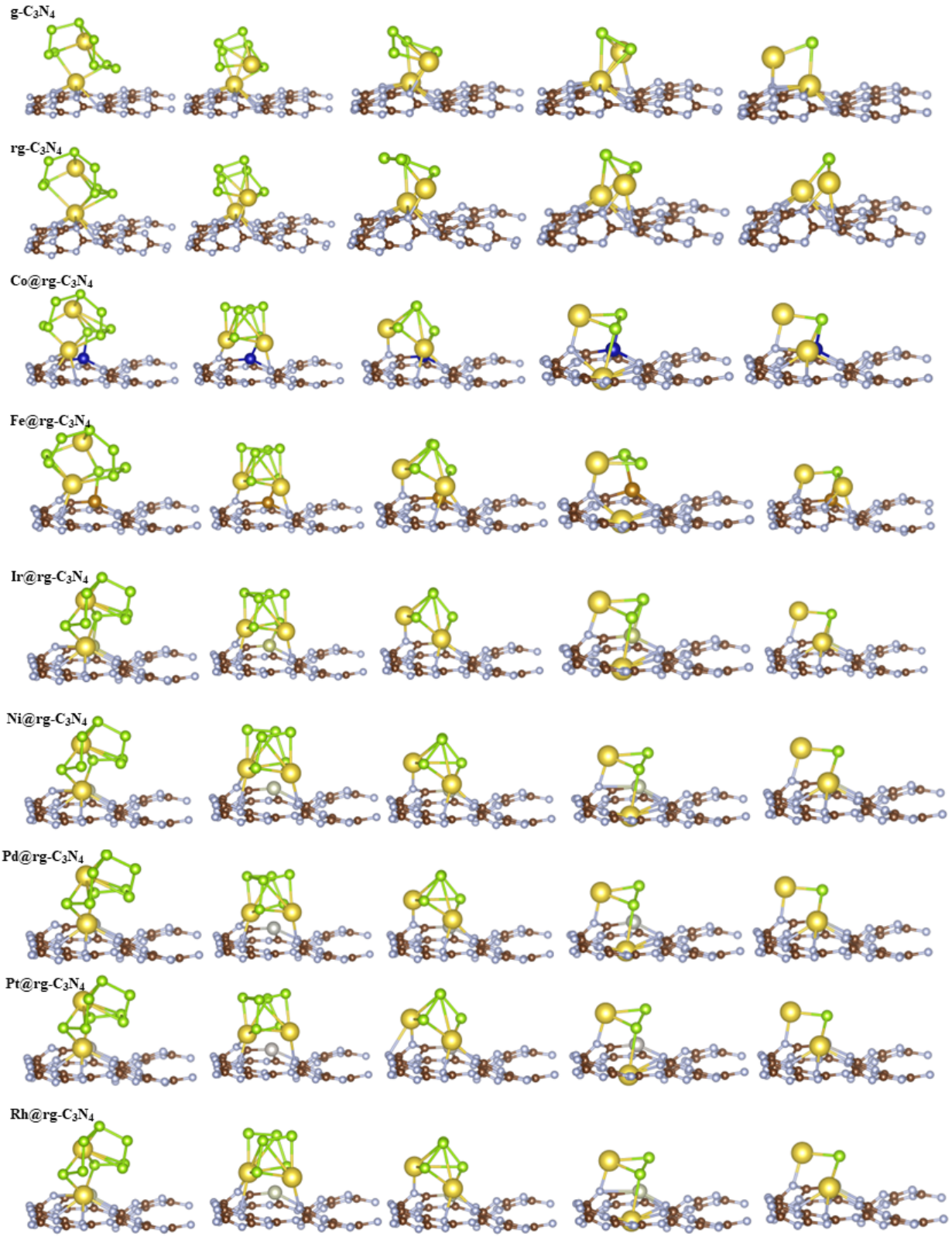

Figure S9: The optimized geometric configurations of Na_2Se_n (n=1, 2, 4, 6, 8) species ong$-C_3N_4$, rg$-C_3N_4$, and SA@rg$-C_3N_4$ (SA = Co, Fe, Ir, Ni, Pd, Pt, and Rh)

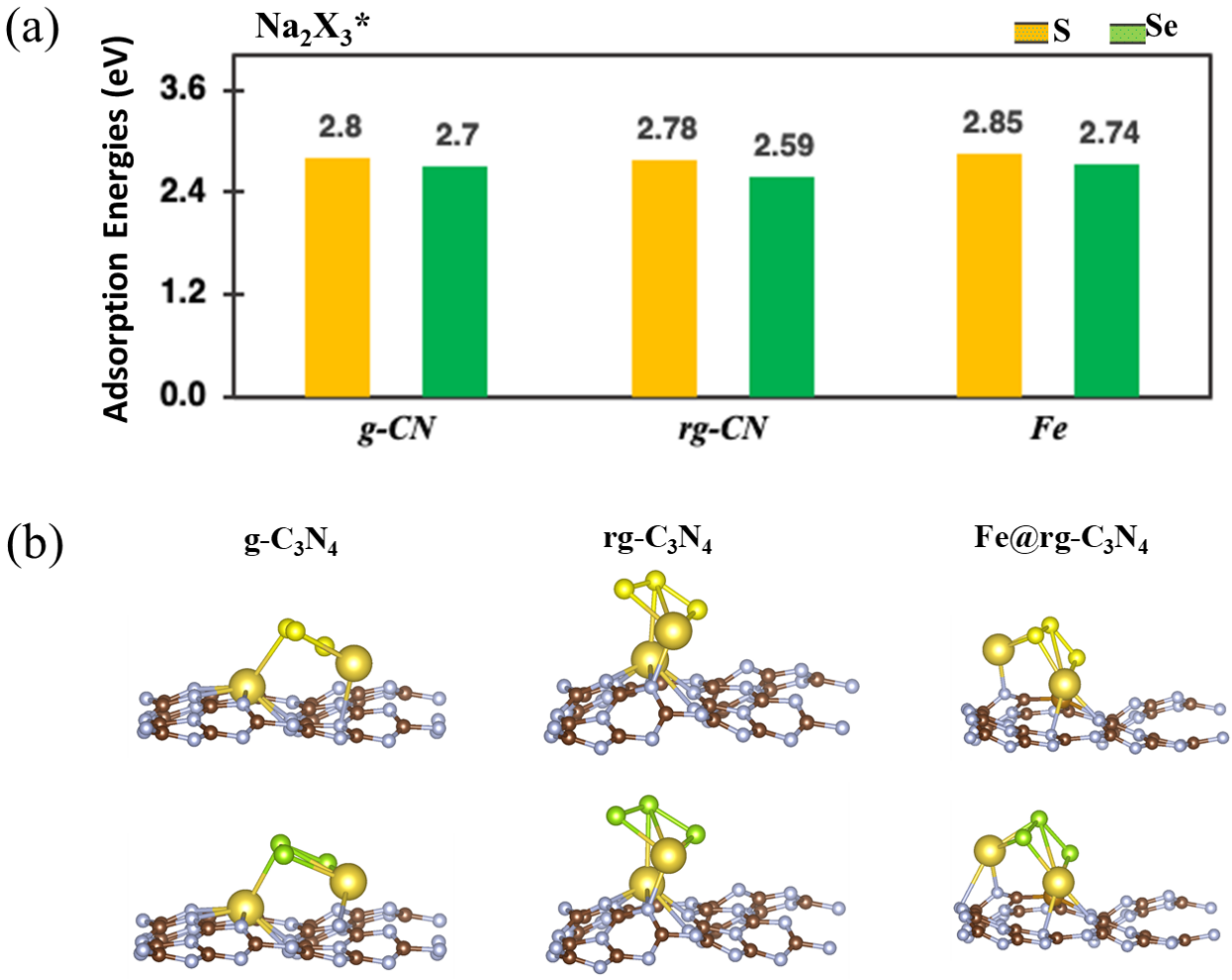

Figure S10: (a)The adsorption energies and (b) optimized geometric configurations of Na_2X adsorbed on Pristine, reduced and Fe@rg$-C_3N_4$

Optimized Geometries of Electrolyte Solvent (DOL and DME)

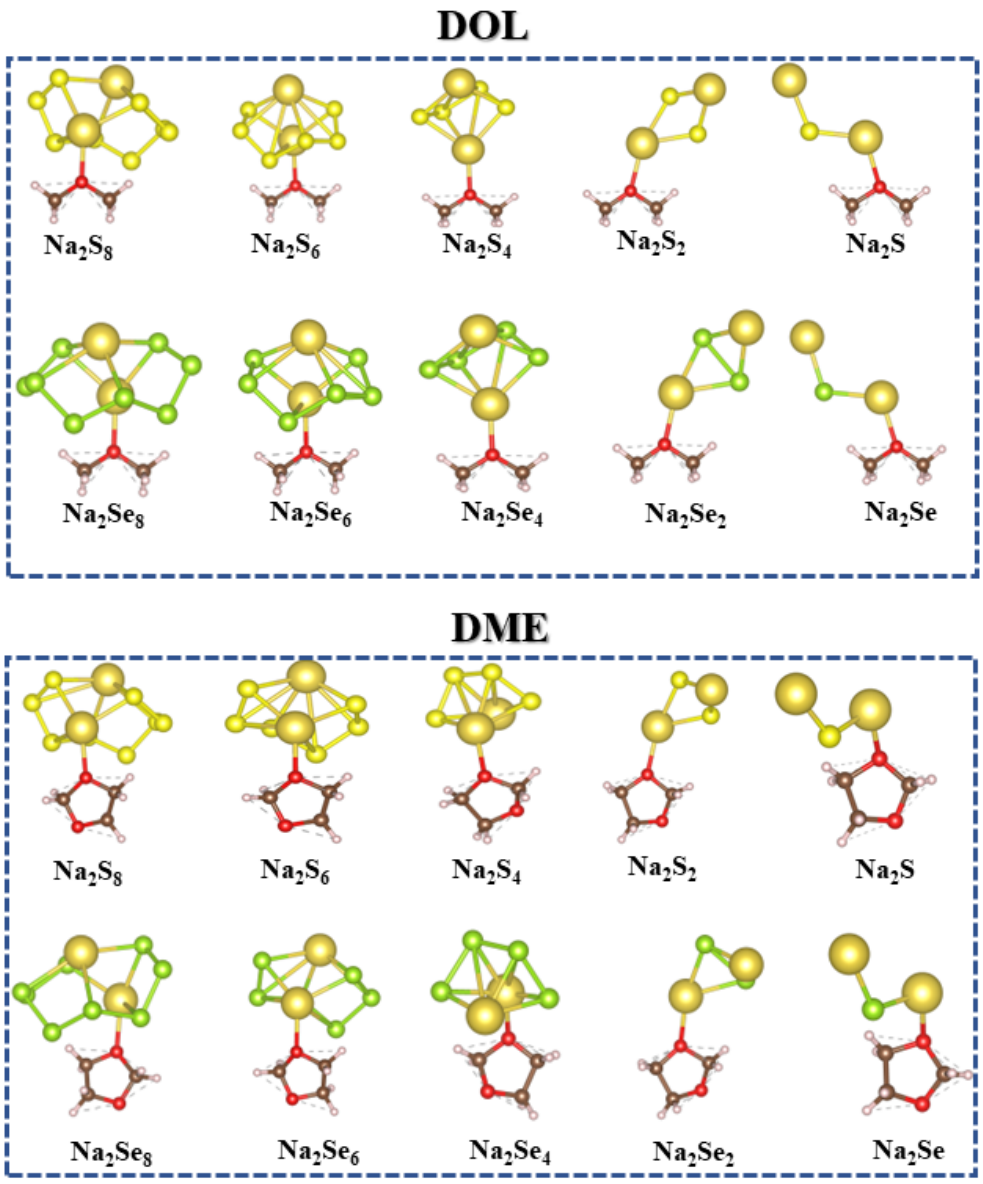

Figure S11: The optimized geometric configurations of Na_2X_n (n=1, 2, 4, 6, 8) species adsorbed on 1,3-dioxolane (DOL) and 1,2 dimethoxymethane (DME) electrolyte solvent

Gibbs free energy profile for sulfur/selenium reduction reaction (S/SeRR)

Overall, the reduction reaction of a sulfur (S_8) or selenium (Se_8) molecule in the discharging process of Na−S or Na−Se batteries is a 16-electron process, resulting in the generation of eight Na_2S or Na_2Se molecules, respectively.[2–4]

$$S_8 + 16Na^+ + 16e^- \rightarrow 8Na_2S$$

$$Se_8 + 16Na^+ + 16e^- \rightarrow 8Na_2Se$$

The elementary steps of forming one Na_2S/Na_2Se molecule in the S/Se reduction reaction (S/SeRR) process are shown as follows, based on a model of Na-pS/Ses disproportional reactions:

$$
\begin{aligned}
{}^*X_8 + 2Na^+ + 2e^- &\rightarrow^* Na_2X_8 \\
{}^*Na_2X_8 &\rightarrow^* Na_2X_6 + \frac{1}{4}X_8 \\
{}^*Na_2X_6 &\rightarrow^* Na_2X_4 + \frac{1}{4}X_8 \\
{}^*Na_2X_4 &\rightarrow^* Na_2X_2 + \frac{1}{4}X_8 \\
{}^*Na_2X_2 &\rightarrow^* Na_2X + \frac{1}{8}X_8
\end{aligned}
$$

where $*$ stands for an active site on the catalytic surface and X= S, Se.

For each step of S/Se reduction reaction (S/SeRR), the reaction Gibbs free energy is given by:

$$\Delta G = \Delta E + \Delta E_{ZPE} - T\Delta S$$

where: ΔE is the total energy calculated from the DFT calculations, ΔE_{ZPE} is the con-

tribution of zero-point energy to the free energy, ΔS is the contribution of entropy to the free energy. The values of ΔE_{ZPE} and ΔS are determined by the vibrational frequency computations, and herein T is the temperature (298.15 K).

The free energy change for the S/SeRR electrochemical steps can be obtained from the following expressions:

$$\begin{aligned}
\Delta G_1 &= (E_{*Na_2X_8} + E_{ZPE(*Na_2X_8)} - TS_{*Na_2X_8}) \\
&\quad - (E_{*X_8} + E_{ZPE(*X_8)} - TS_{*X_8}) - 2(E_{Na} + E_{ZPE(Na)} - TS_{Na}) \\
\Delta G_2 &= (E_{*Na_2X_6} + E_{ZPE(*Na_2X_6)} - TS_{*Na_2X_6}) \\
&\quad - \frac{1}{4}(E_{X_8} + E_{ZPE(X_8)} - TS_{X_8}) - (E_{*Na_2X_8} + E_{ZPE(*Na_2X_8)} - TS_{*Na_2X_8}) \\
\Delta G_3 &= (E_{*Na_2X_4} + E_{ZPE(*Na_2X_4)} - TS_{*Na_2X_4}) \\
&\quad - \frac{1}{4}(E_{X_8} + E_{ZPE(X_8)} - TS_{X_8}) - (E_{*Na_2X_6} + E_{ZPE(*Na_2X_6)} - TS_{*Na_2X_6}) \\
\Delta G_4 &= (E_{*Na_2X_2} + E_{ZPE(*Na_2X_2)} - TS_{*Na_2X_2}) \\
&\quad - \frac{1}{4}(E_{X_8} + E_{ZPE(X_8)} - TS_{X_8}) - (E_{*Na_2X_4} + E_{ZPE(*Na_2X_4)} - TS_{*Na_2X_4}) \\
\Delta G_5 &= (E_{*Na_2X} + E_{ZPE(*Na_2X)} - TS_{*Na_2X}) \\
&\quad - \frac{1}{8}(E_{X_8} + E_{ZPE(X_8)} - TS_{X_8}) - (E_{*Na_2X_2} + E_{ZPE(*Na_2X_2)} - TS_{*Na_2X_2})
\end{aligned}$$

The largest ΔG will determine the overall speed of the Na–X battery reaction, and the corresponding reaction step is called rate determining (RD) step.

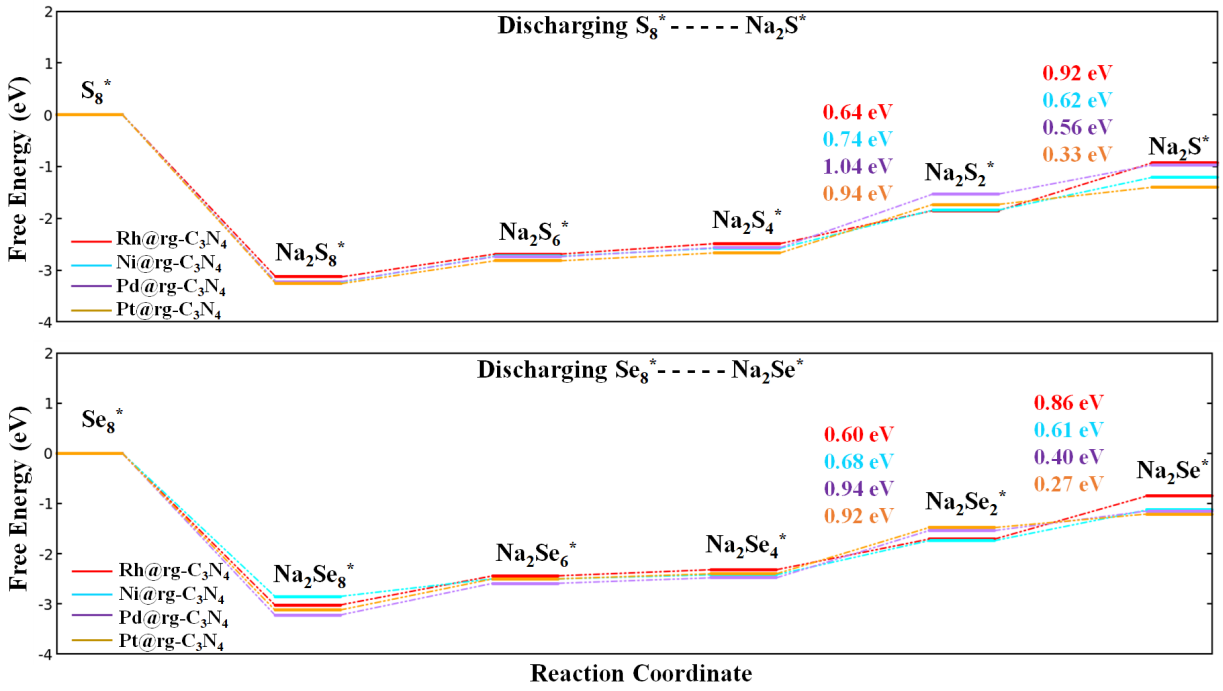

Figure S12: Energy profiles for the reduction of Na-pXs (X= S, Se) on the SA@rg$-C_3N_4$ (SA= Rh, Ni, Pd and Pt) monolayer.

Partial Density of States (PDOS) of Na_2X-SA

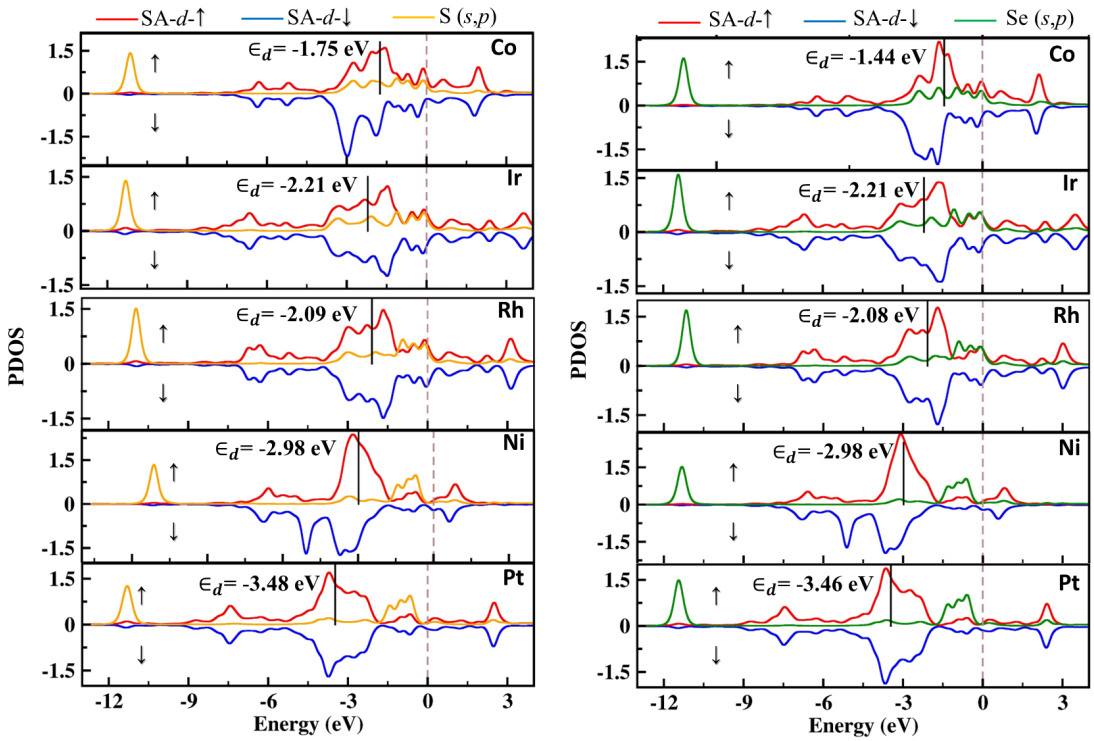

Figure S13: The calculated partial density of states (PDOS) of Na_2X-SAC (Co, Ir, Rh, Ni and Pt) adsorption system

References

(1) Li, N.; Zhan, Y.; Wu, H.; Fan, J.; Jia, J. Covalent surface modification of bifunctional two-dimensional metal carbide MXenes as sulfur hosts for sodium–sulfur batteries. *Nanoscale* **2022**, *14*, 17027–17035.

(2) Wei, C.; Ge, M.; Fang, T.; Tang, X.; Liu, X. Rational design of MXene-based single atom catalysts for Na–Se batteries from sabatier principle. *Physical Chemistry Chemical Physics* **2023**, *25*, 24948–24959.

(3) Jayan, R.; Islam, M. M. Mechanistic Insights into Interactions of Polysulfides at VS2 Interfaces in Na–S Batteries: A DFT Study. *ACS Applied Materials & Interfaces* **2021**, *13*, 35848–35855.

(4) Assary, R. S.; Curtiss, L. A.; Moore, J. S. Toward a molecular understanding of energetics in Li–S batteries using nonaqueous electrolytes: a high-level quantum chemical study. *The Journal of Physical Chemistry C* **2014**, *118*, 11545–11558.